Raman bands of double-wall carbon nanotubes: comparison with single- and triple-wall carbon nanotubes, and influence of annealing and electron irradiation

Pascal Puech, Emmanuel Flahaut, Ayman Bassil, Thomas Juffmann, François Beuneu, Wolfgang Bacsa

DOI: 10.1002/jrs.1690

Raman bands of double-wall carbon nanotubes: comparison with single- and triple-wall carbon nanotubes, and influence of annealing and electron irradiation

P. Puech,[1]* E. Flahaut,[2] A. Bassil,[1] T. Juffmann,[1] F. Beuneu[3] and W. S. Bacsa[1]

[1] Laboratoire de Physique des Solides de Toulouse, UMR-CNRS 5477, Université Paul Sabatier, 118 Route de Narbonne, 31062 Toulouse, France
[2] CIRIMAT-LCMIE, UMR-CNRS 5085, Université Paul Sabatier, 118 Route de Narbonne, 31077 Toulouse cedex 4, France
[3] Laboratoire des solides irradiés, Ecole Polytechnique, 91128 Palaiseau Cedex, France

We compare the G and G'_{2D} bands of single-, double- and triple-wall carbon nanotubes (CNTs). We observe that the band shape is sensitive to the number of walls of the CNTs. For single-wall carbon nanotubes (SWCNTs), the G band is composed of two distinct contributions G+ and G−, while the G band for double-wall nanotubes is composed of one band with two main contributions from the inner and the outer tube. The G'_{2D} band can be fitted with one Lorentzian for single-wall tubes, while two distinct contributions are observed for double-wall carbon nanotubes (DWCNTs). Considerable variations of the G'_{2D} band are found with similar first order Raman spectra. Annealing influences the D- and RBM-band intensities. Electron irradiation has the effect of decreasing the G- and D-band wavenumbers but does not enhance the D-band intensity considerably. The down-shifts of the G- and D-band wavenumbers are correlated and are the same for two excitation wavelengths. This is consistent with the scattering of phonons around the K-point.

KEYWORDS: Raman; nanotubes; double wall; defects

INTRODUCTION

Carbon nanotubes (CNTs) continue to attract much attention owing to the large number of their potential applications such as in electronic circuits, polymer composites for electrostatic charge dissipation and mechanical reinforcement.[1] The Raman signals from single-wall carbon nanotubes (SWCNTs) have been studied in great detail. The Raman spectrum of CNT consists of bands at low energy range, due to the radial breathing modes (RBM) sensitive to the diameter and chirality/helicity for small diameter tubes.[2] The RBM bands are particularly sensitive to the excitation wavelength with narrow resonance profiles (<100 meV)[3,4] and with a small broadening and energy shift when in bundles.[5] Raman as well as photoluminescence studies show that it is possible to determine the tube chirality/helicity by varying the excitation wavelength and locating the resonances that are directly related to electronic transition energies characteristic for each chirality/helicity for suspended tubes embedded in surfactants in aqueous solution.[6] The dispersive D band has been shown to be related to defect-induced double resonant scattering processes that involve elastic scattering of electrons by structural defects and is often used to assess the quality of CNTs.[7,8] The G mode in SWCNTs, near the position of the G mode in graphite, consists of two bands at 1590 cm^{-1} (G+) and at around 1572 cm^{-1} (G−) for tubes with a diameter of 1.4 nm. The position of the G+ mode is not sensitive to the tube diameter. The precise position of the G band depends on the diameter (C/d^2, C: a constant depending on the semiconducting or metallic behaviour; d: the diameter).[9] Coupling with valence electrons in metallic CNTs has a strong influence on the band shape and the intensity of the G bands.[10] For multi-wall carbon nanotubes (MWCNTs), the number of walls and the presence of faceted graphitic particles complicate the G-band intensity and band shape. RBMs are only rarely observed, but the D band is often present and is broadened. On the higher wavenumber side of the G band, a shoulder due to the so-called D′ band is sometimes observed.[11]

*Correspondence to: P. Puech, Laboratoire de Physique des Solides de Toulouse, UMR-CNRS 5477, Université Paul Sabatier, 118 Route de Narbonne, 31062 Toulouse, France.
E-mail: puechp@lpst.ups-tlse.fr

Double-wall carbon nanotubes (DWCNT) are the simplest form of MWCNT. Two synthesis routes have been reported. The conversion of SWCNTs filled with C_{60} molecules (peapods), which can be transformed into DWCNTs, leads to a narrow distribution of the internal and external diameters of the tubes.[12] Catalytic hemical vapour deposition (CCVD) is the second method to grow DWCNTs with a larger distribution of diameters.[13] Inter-layer coupling between the two walls in DWCNTs has been investigated for RBMs using resonant Raman scattering.[14] Hydrostatic pressure experiments on DWCNT's[15,16] show that the G band splits with pressure. The wavenumber at zero pressure of the inner tube is close to 1582 cm^{-1} while the wavenumber of the outer tube is close to 1592 cm^{-1}. The wavenumbers of both the inner and outer tubes have been estimated earlier using doped DWCNTs.[17] While the G-band shape from DWCNTs obtained with peapods changes with the excitation energy, DWCNTs grown by the CCVD method are less sensitive to the excitation energy.[18]

Doping influences the population of the electronic states and leads to charge transfer. Electron acceptors such as H_2SO_4 (Ref. 19), Br_2 (Ref. 17) or CrO_4 (Ref. 20) have been used, and shifts to higher energies have been observed for all the spectral bands. For H_2SO_4, Br_2 and CrO_4, the shift of the G+ band is 16, 19 and 24 cm^{-1}, respectively, while the shift of the G'_{2D} band is 12 cm^{-1} for H_2SO_4 and 40 cm^{-1} for CrO_4. It is observed that the intensity of the G'_{2D} band decreases when CNTs are in contact with acceptors. For electron donors, such as Ag (Ref. 20), the down-shift can be as large as -9 cm^{-1} for the G+ band and -10 cm^{-1} for the G'_{2D} band. For DWCNTs, doping effects have also been reported[17,20] and intensity transfer from the G band, associated with the outer tube, to other spectral bands have been suggested.[15,21] The D band contains several spectral components related to the double resonant process and the presence of Van Hove singularities in CNTs.[22] The second-order spectrum of the D band, G'_{2D}, has been used to probe the effects of the environment on SWCNTs.[23,24] It has been suggested that the two features contributing to the D band are due to the inner and outer tubes,[25] leading, consequently, to a splitting of the G'_{2D} band. Its temperature and pressure dependence are useful to extract information on the influence of the tube environment. Although the intensity of the D band is used to assess the quality of the sample, one has to keep in mind that the ratio of the D- and G-band intensities is strongly wavelength dependent. Furthermore, it has been observed that the intensity of the D band is correlated to the RBM intensity as long as the defect density is not too high.[26]

In this paper, we first present experimental studies to show how the shape of the G band changes with the number of walls and discuss in detail the origin of these differences. Then, we carry out a statistical analysis of the intrinsically inhomogeneous system to draw general conclusions on the Raman spectra of DWCNTs. The samples we studied were composed of tubes with a large size distribution, with diameters ranging from 0.5 to 3 nm. We recorded the spectra from a large number of spots on the surface dispersed sample and we carried out a statistical analysis of the recorded spectral bands. We alo implanted defects by electron irradiation to observe their influence on the D-band wavenumber and intensity. Finally, we summarize the evolution of the G and D band in DWCNTs as a function of temperature and pressure and make a comparison with the graphite.

EXPERIMENTAL

Arc-prepared SWCNT were supplied by NANOCARBLAB, with a narrow diameter distribution centred at 1.4 nm. DWCNTs were prepared by CCVD.[13] High-resolution electron microscopy images show the presence of individual and small bundles of DWCNTs with radii ranging from 0.3 to 1.5 nm. The tubes are single- (15%), double- (80%) or triple-walled (5%). Small changes in the catalyst composition (replacing Mo by W) lead to a sample with 50% tripled-wall CNT (TWCNT), 35% DWCNTs and a few four-walled CNTs.[27] In the following, this latter sample is referred to as TDWCNTs. Thermal annealing in air at 450 °C results in the removal of graphitic carbon on the CNTs and reduction of the D-band intensity. In order to distinguish CNTs with this soft annealing, we denote the heated samples with 'h'. Annealing of DWCNTs (a-DWCNTs) to higher temperatures (600 °C)[18] leads to a strong reduction in intensity and eventual disappearance of the D band. Oxidation of CNTs reduces the sample weight substantially. DWCNTs have been irradiated (i-DWCNT) by 2.5-MeV electrons at a dose of 0.74 C/cm^2. Highly oriented pyrolytic graphite (HOPG) was used as the reference. The first series of measurements was carried out using a Renishaw spectrometer with low laser power (3 $\mu W/\mu m^2$ on the sample) to avoid heating using the 514.5-nm line of an argon ion laser. The measurements on h-DWCNT, a-DWCNT and i-DWCNT were carried out with a visible Dilor spectrometer using Ar or Kr ion lasers. All the measurements were made at room temperature using the backscattering geometry. Great care was taken to avoid heating effects by the laser irradiation.

G and G'_{2D} band shapes and influence of the surrounding medium

We first consider the G and G'_{2D} bands and study the influence of methanol on the vibrational bands of the different types of CNTs. Figure 1 shows the G band and the G'_{2D} band of SWCNTs, DWCNTs, TDWCNTs and graphite. The spectra of the tubes in air are drawn in bold lines and those of the tubes in methanol with a thin line. Low laser power was used to prevent the movement of the sample in methanol due to laser heating. We first discuss the spectra in air. For the SWCNT spectrum, we find the usual G+ band at 1590 cm^{-1} and the G-band at 1570 cm^{-1}. Using

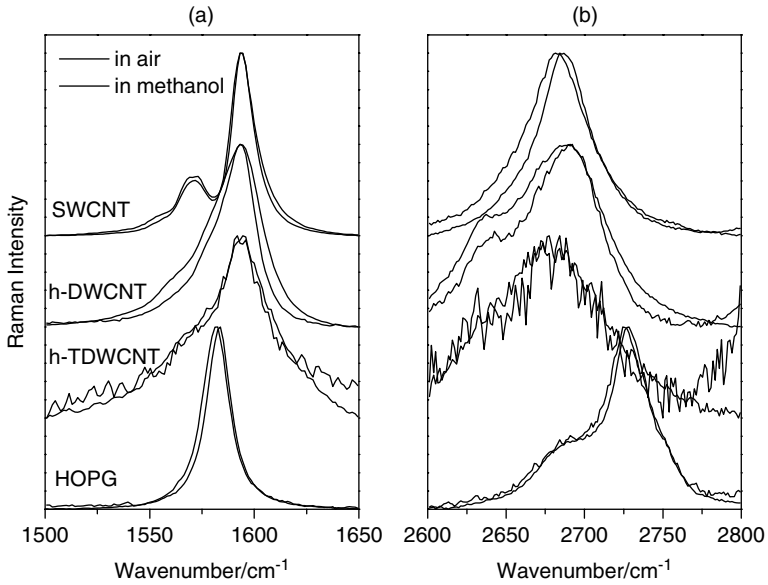

Figure 1. Typical Raman spectra of several species in the G- and G'_{2D}-band range in air (bold line) and in methanol (thin line) with very low laser power at 514.5 nm.

the 514.5 nm laser excitation, the photon energy falls in the range of the E_{44}^{SC} transition for semiconducting tubes.[8] Both wavenumbers are in agreement with previous reports.[8] For the DWCNT spectrum, we find a single broader G band. This can be explained using the observations of the G band under hydrostatic pressure, which reveal a G band for the inner tube at 1582 cm^{-1} and a band for the outer tube at 1592 cm^{-1}. The shape of the G band is in agreement with previous reports[25–29] but differs slightly from that of the DWCNTs obtained using the peapod method.[30] The G bands of the inner and outer walls in DWCNTs are close in wavenumber and are difficult to separate at normal pressure. The full width at half-maximum for each peak, considering contributions from the inner and outer tubes, is the same when compared to SWCNTs (14–16 cm^{-1}). It is interesting to note that the line shape is asymmetric towards the low wavenumber side. For the TDWCNT sample, the G band is larger and more asymmetric. For HOPG, a single Lorentzian band is located at 1582 cm^{-1}. From these observations, we conclude that distinct differences exist between SWCNTs and DWCNTs. With increasing number of walls (MWCNTs) the differences are reduced[11] and the G band shows a line shape that is intermediate between those of DWCNTs and graphite. The G band corresponding to the outer walls is located towards higher wavenumbers. The external wall is particularly sensitive to doping and the reported G-band shift is high for SWCNTs, while a change in line shape is observed for DWCNTs. We discuss here the results in methanol, which is a medium with no doping effect. In Fig. 1(b), we report the Raman spectra associated with the G'_{2D} band. For SWCNTs, we observe a single peak, whereas for graphite the same band has a clear shoulder and is up-shifted in energy. A single sheet of graphene gives a Lorenzian line shape. The wavenumber dependence *vs* the wavelength (100 cm^{-1}/eV) and diameter of the G'_{2D} band has been reported earlier.[31] The DWCNT spectrum also shows a shoulder. The TDWCNT spectrum shows one broad G'_{2D} band. All the observed G'_{2D} bands fall in the 2630–2700 cm^{-1} interval. Two contributions to the G'_{2D} band have been reported,[32] as well as contributions from inner and outer tubes located at different wavenumbers for the D band.[25] The broad TDWCNT spectrum is close to that found for MWCNT.[11] G-band shape changes are reported while doping,[19] applying pressure[21] and changing the surrounding medium.[23] The influence of the environment on the G band might be unexpected at first. But all carbon atoms of SWCNTs are on the surface and, as a result, the G band is sensitive to the environment. Large shifts (20 cm^{-1}) of the G'_{2D} band in SWCNTs have been reported in the literature.[23] We compare spectra of CNTs in methanol and air when using a low laser power (Fig. 1). We observe that the band positions change slightly. No significant charge transfer is expected for methanol. The G'_{2D} band shift has been used by several authors to sense the modification of the tube environment.[33–35] For SWCNTs, the bundles are believed to be compact owing to their narrow diameter distribution and, consequently, the medium does not penetrate the bundle. For DWCNTs, no effect is observed due to the medium. The presence of the inner tube reduces the influence of the observed spectral lines on the surrounding medium. We note that we use here a very low laser power to prevent any heating. CNTs absorb light polarised along the tube axis. A higher temperature increases the interaction with the medium and this can explain the discrepancy in the results reported here and by Wood *et al*.[23]

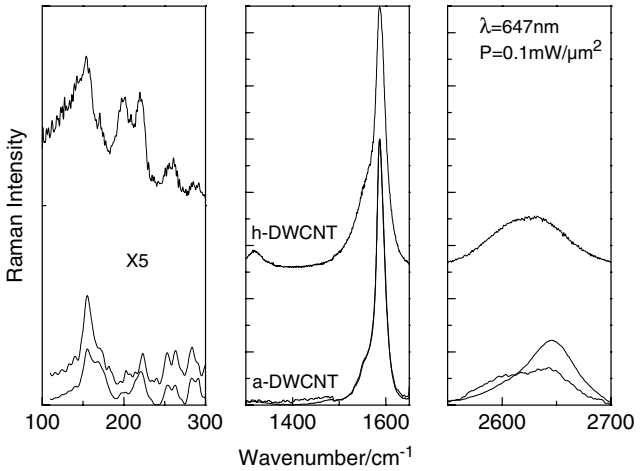

Figure 2. Spectra from two different locations within the same annealed sample of DWCNT (a-DWCNT) and a reference spectrum of h-DWCNT.

Effect of annealing on RBM, G and G′$_{2D}$ band

Thermal annealing modifies the Raman spectra of CNTs. We compare here the modifications observed in the spectral bands of DWCNTs after annealing. Figure 2 shows one spectra after a thermal annealing at lower temperature (450 °C, h-DWCNT) and at a higher temperature (600 °C, a-DWCNTs). All spectra in Fig. 2 were recorded using the 647-nm excitation. The two a-DWCNT spectra in Fig. 2 have been acquired on the same sample at two different locations. The disappearance of the D band after annealing proves that defective regions are oxidized by annealing.[17] The observation of RBMs with similar intensities shows that the diameter distribution probed at 647 nm has not changed. Comparing this with h-DWCNTs, we observe that annealing at a higher temperature increases the intensity of the RBMs of smaller diameter tubes (>250 cm^{-1}) and that the G-band asymmetry at the low wavenumber side is reduced. From this, we would expect an intense G′$_{2D}$ band. Although the RBM and G bands are similar, we observe a clear difference in the G′$_{2D}$ band for the two locations on the sample. This demonstrates that one has to be cautious about drawing conclusions from the G′$_{2D}$-band intensity and shows that statistical analysis of a larger number of spectra might be useful to draw conclusions about heterogeneous samples. In hydrostatic pressure experiments, it is observed that the G′$_{2D}$ band disappears at a relatively low pressure (3 GPa). The G′$_{2D}$ band has two components using 633-nm excitation, a band located at 2600 cm^{-1} that shifts with pressure by roughly half the amount of the band located (P Puech, W Bacsa, H Huebel, A Sapelkin and DJ Dunstan, Private communication) at 2650 cm^{-1}. This is in agreement with the assignment of one band to the inner tube and the other to the outer tube. Assignments to the inner and outer tube have also been reported for the D band.[25] Using spectroscopic mapping, we can probe whole regions and treat the spectra numerically for statistical data analysis. This strategy, however, is not simple to implement with the G′$_{2D}$ band, and the correlation with the intensity of D is not simple. We believe that resonance effect is at the origin of the observed variation of the G′$_{2D}$-band intensity. Two components are believed to contribute. For DWCNTs, the wavenumber can vary between the two limits given by the wavenumber corresponding to the inner tube and the outer tube.

The effect of electron irradiation on the D band

Electron irradiation creates point defects in the sp^2-bonded CNT walls. The D band is often used to characterize the defect density in CNTs and graphite. The ratio of the D-band intensity to that of the G band or G′$_{2D}$ band is often used[34] as a relative measure of the defect density. For a highly defective sample, this approach gives satisfactory qualitative results, whereas when using a high-quality sample this relation is less clear. The D band can be in resonance, and as a result the G band intensity depends on the excitation wavelength. The D-band intensity is also found to be sensitive to doping,[20] which also influences the intensity ratio. Probing a large diameter distribution and resonance conditions depending on diameter and using spectroscopic mapping, we can have better insight into the effect of electron irradiation on the creation of defects and their influence on the D-band intensity. The defect-induced Raman process responsible for the D band consists of four steps: excitation of an electron–hole pair, inelastic scattering of the electron (or hole) by phonons at the zone boundary, elastic scattering of an electron (or hole) by a defect and recombination of the excited electron and hole.[7] For CNTs, the D band is sensitive to Van Hove singularities.[22] Sato *et al*.[35] have shown for graphitic materials that the D/G intensity ratio decreases with increasing energy of the exciting radiation. Figure 3 shows two spectra of i-DWCNTs obtained with the 568-nm excitation. The spectra shown are from two different locations on the DWNT sample. To simplify the fitting process and the discussion, we fitted the band with a single Lorentzian. The linewidth of both D and G bands remains the same, but we observe a clear down-shift with irradiation on some spots on the sample. One can notice that the intensity of the D band does not become higher even though the down-shift is large. To follow the variation of the D-band intensity as a function of the down-shift of the D band, we have plotted in the same figure the I_D/I_G intensity ratio *vs* the D-band wavenumber and incorporated the results obtained on h-DWCNT. The small intensity of the D band for the a-DWCNTs cannot be fitted by a Lorenzian and is not considered in the following. Interestingly, no correlations exist between the down-shift and the intensity. The defects introduced by high-energy electrons (2.5 MeV) are not efficient in scattering the excited electrons as needed in the double-resonance process. For nanotubes of very small diameter embedded in a zeolite PO_4 matrix and graphitic nano-particles, a strong D-band resonance can

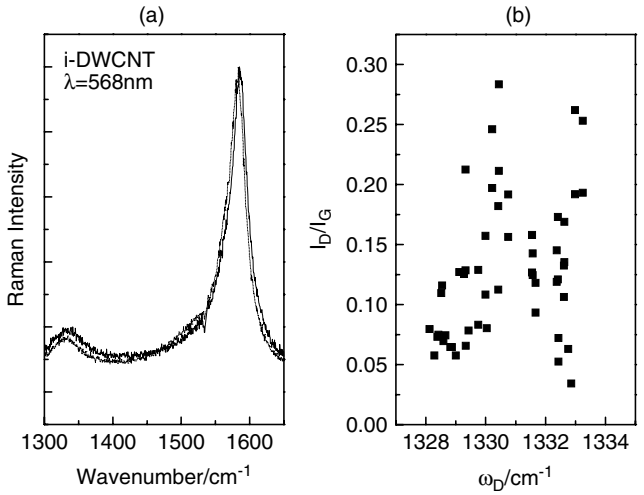

Figure 3. The spectra from two different locations with the same heterogeneous sample of i-DWCNT (a) and mapping of I_D/I_G intensity ratio as a function of the wavenumber ω_D (b).

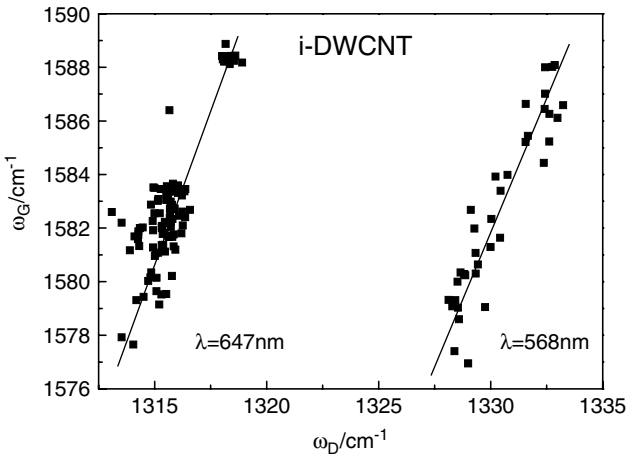

Figure 4. Mapping of ω_D and ω_G wavenumbers of i-DWCNT probed at two wavelengths.

lead[36,37] to a D/G ratio of higher than 1. Clearly, the D band is not in resonance in the spectra shown in Fig. 3. We have observed previously that the D-band intensity increases after a pressure cycle.[38] This suggests that defects are created by applying a high pressure, and are active in the scattering process related to the D band, while the point defects created by irradiation are inefficient in the scattering process. It has been reported[39] earlier that defects created by electron irradiation can form bridges to coalesce the CNTs. We observe that the i-DWCNT samples do not disperse using sonication after the electron irradiation. The small D band results in a D/G intensity ratio of smaller than 0.2 with 647-nm excitation and 0.3 with 568-nm excitation. The created defects down-shift the wavenumber of both the D and the G band.

In Fig. 4 we show the correlation of the G and D band positions for a set of spectra recorded at different locations of the sample, as well as data for h-DWCNTs, for fixing the limit in the higher wavenumber range. The G-band position is as low as 1577 cm^{-1} and is the same for the two different excitation wavelengths. The slope, which shows the correlations for the two bands, is the same within experimental error. Again we used external laser powers below 1 mW (<0.1 mW on the sample) to exclude any heating effects. We note that both the excitation wavelengths used here are not strongly absorbed.[26] A decrease of 10 cm^{-1} would correspond to a heating of approximately 500 °C. But we do not observe any broadening, which should be present if heating does occur. We estimate a broadening of 15–23 cm^{-1} for a temperature increase of 500 °C. Although the presence of defects might reduce the thermal conductivity, we conclude that heating effects are not important here. The wavenumber decrease is associated with a phonon softening of the pristine sp^2-bonded lattice. The wavenumber of the G band and the wavenumber of the phonons in the K–M phonon branch involved in the double resonant process have the effect of down-shifting the D band and our experimental observation gives a value of 0.5 when comparing the down-shifts of the D and G bands. The lack of a strong resonance shows clearly that not all defects scatter in the same way. It is not clear at this point which type of defects is efficient in the double-resonance Raman process. We find no correlation between the down-shift of the wavenumbers and the intensity of the D band. We conclude that it is not sufficient to use the D/G intensity ratio. Our experimental results show that the defects created by high energetic electrons down-shift the wavenumber without strongly increasing the D-band intensity.

Summary of pressure- and temperature-induced effects of the D and G bands in DWCNTs

We compare the results found here with those reported in the literature. The results are summarized in Table 1. We notice that the reported literature values are spread considerably. The spread can be attributed to the various synthesis methods used and the different experimental conditions. It appears that the data for DWCNTs are spread less; the tube diameters fall in the same range. DWNTs obtained through peapods conversion have a mean outer tube diameter of 1.4 nm, while using the CCVD method the mean outer tube diameter is around 2 nm. The coupling of the tubes can be observed[14] in RBMs, where very narrow peaks can appear above 300 cm^{-1}. Interestingly, the RBM intensity does correlate with that of the D band, showing similarity in the resonant process for the two types of bands. The G band in DWCNTs is composed of at least three bands.[21] Hydrostatic pressure is useful to study the composition of the G band. The two components behave differently when applying pressure. Br_2 doping is another way to observe the contributions from inner and outer tubes. The signal from the outer tube is considerably reduced for the G band and for the RBMs.[17]

Table 1. Pressure and thermal phonon parameters

	$\frac{\partial\omega_G}{\partial P}$ (cm^{-1}/GPa)	$\frac{\partial\omega_D}{\partial P}$ (cm^{-1}/GPa)	$\frac{\partial\omega_G}{\partial T}$ (cm^{-1}/K)	$\frac{\partial\omega_D}{\partial T}$ (cm^{-1}/K)
SWCNT	4–8[40]	$0.5\frac{\partial\omega_G}{\partial P}$ [26]	−0.023[41] to −0.04[42]	−0.019[41]
DWCNT	inner = 3.1[15,16] outer = 5.6	–	−0.022[28,43] to −0.026[18]	−0.014[18]
MWCNT	4.3[44] −6.6[45]	–	−0.028[41]	−0.018[41]
Graphite	4.8[46]	–	−0.028[47]	−0.019[47]

For the D band, it was shown that the band is diameter-sensitive, and in the case of DWCNs one can expect a contribution from both inner and outer tubes, located at different wavenumbers. Unfortunately, the splitting at lower pressures cannot be followed with a diamond pressure cell because of the Raman signal from diamond and the fact that the D band disappears[26] at around 3 GPa. In the DWCNT samples used here, the large diameter distribution leads to a contribution that can be fitted with a single Lorentzian, while with DWCNTs obtained from peapods, the D-band shape is due to a double contribution.[25] To have an accurate value of the temperature dependence, we immersed the DWCNTs in methanol and then placed the cell filled with methanol in a cryostat. Methanol is a liquid between −97 and 65 °C and we have obtained a linear variation in this temperature range. The fitting procedure is not trivial when there are too many contributions within a single band. We have fitted our data for the temperature dependence of the G band with two contributions and found the same results for the inner and outer tubes. The variation of the splitting between the wavenumber of the inner and the outer tube is small within the investigated temperature range. As a consequence, we report the average value in Table 1. For the D band, the values reported are not fully satisfactory, as the band from a sample with fewer defects has low intensity and consequently the accumulation time needed to obtain a low-noise spectrum is long. On average, the down-shift of the D band due to heating is $-0.013\ cm^{-1}$/K, which can be compared with the value for the G band of about $-0.024\ cm^{-1}$/K. This value is very close to the values for graphite. For SWCNTs and for MWCNTs, similar values have been reported. We can conclude that the thermal expansion of sp^2-bonded carbon is similar.

High-pressure results on SWNTs have been summarized by Loa.[40] Fewer high-pressure reports appeared[44] on MWCNTs probably because of their similarity with graphite. The large diversity of reported data for SWCNTs can be attributed to differences in their syntheses. If the bundle is compact, faceting can occur,[48] which is metastable.[49] Theory shows that elliptical deformation is energetically favourable. Flattening of the tubes is a transition observed for a large diameter range[45] and is predicted[50] to vary as $1/d^3$. For DWCNTs[15,16] several calculations have shown a small reinforcement of the tube and a transition to the elliptical shape as is observed for SWCNTs (Table 1). Several reports consider ordered layers of the medium on the CNT surface to explain the presence of plateaus or the slope *vs* the pressure curve.[21,51] In a recent work, we have used argon, methanol–ethanol mixture and oxygen as the pressure transmitting medium. Oxygen has a clear doping effect, leading to an increase of the G-band wavenumber by $4\ cm^{-1}$ for the outer tube and $2\ cm^{-1}$ for the inner tube. This can be explained by the finite-size effect of the atom/molecule of the pressure medium and the formation of ordered layers. These effects are new, and more investigations are needed to discriminate all the influencing factors. Finally, we note that the D-band intensity is only partially reversible after a pressure cycle. This indicates an incomplete reversibility of the flattening.[38]

CONCLUSIONS

The line shape of the G band of DWCNTs is different from that of SWCNTs and is composed of at least two contributions, one attributed to the inner tube around $1582\ cm^{-1}$ and the other to the outer tube at a higher wavenumber from 1590 to $1594\ cm^{-1}$ depending on the DWCNT sample. A broad contribution at the lower wavenumber side of the G band is also observed. We find that the shape of the G band is an indication of the nanotube type and the interaction of the outer tube with the surrounding molecules, which can be used to probe the species in contact and to observe doping effects. To explore the D-band intensity, we created defects by electron irradiation. We observed clear down-shifts of both the D and the G bands but no increase in the D-band intensity. Furthermore, we find that defects created by pressure cycles enhance the D-band intensity. We conclude that the D band is related to a particular type of defect. While the temperature variation of Raman bands in CNTs is similar to that observed in graphite, the pressure variation of the Raman bands for CNTs is different to that in graphite owing to their cylindrical structure. Future calculations of the phonon deformation potential of the K–M phonon branch would be useful for comparisons with the experimental observations shown here.

REFERENCES

1. *Carbon Nanotubes*. O'Connell MJ (ed.). CRC Taylor and Francis EAN13 number : 9780849327483, 2006.
2. Rao AM, Richter E, Bandow S, Chase B, Eklund PC, Williams KW, Menon M, Subbaswamy KR, Thess A, Smalley RE, Dresselhaus G, Dresselhaus MS. *Science* 1997; **275**: 187.

3. Telg H, Maultzsch J, Reich S, Hennrich F, Thomsen C. *Phys. Rev. Lett.* 2004; **93**: 177401.
4. Fantini C, Jorio A, Souza M, Strano MS, Dresselhaus MS, Pimenta MA. *Phys. Rev. Lett.* 2004; **93**: 147406.
5. O'Connell M, Sivaram S, Doorn S. *Phys. Rev.* 2004; **B69**: 235415.
6. Bachilo SM, Strano MS, Kittrell C, Hauge RH, Smalley RE, Weisman RB. *Science* 2002; **298**: 2361.
7. Maultzsch J, Reich S, Thomsen C. *Phys. Rev., B* 2004; **70**: 155403.
8. Sato K, Saito R, Oyama Y, Jiang J, Cançado LG, Pimenta MA, Jorio A, Samsonidze GeG, Dresselhaus G, Dresselhaus MS. *Chem. Phys. Lett.* 2006; **427**: 117.
9. Jorio A, Souza Filho AG, Dresselhaus G, Dresselhaus MS, Swan AK, Ünlü MS, Goldberg BB, Pimenta MA, Hafner JH, Lieber CM, Saito R. *Phys. Rev., B* 2002; **65**: 155412.
10. Lefrant S, Baltog I, Baibarac M, Schreiber J, Chauvet O. *Phys. Rev., B* 2002; **65**: 235401.
11. Cui S, Canet R, Derre A, Couzi M, Delhaes P. *Carbon* 2003; **41**: 797.
12. Bandow S, Takizawa M, Hirahara K, Yudasaka M, Iijima S. *Chem. Phys. Lett.* 2001; **337**: 48.
13. Flahaut E, Bacsa R, Peigney A, Laurent C. *Chem. Commun.* 2003; **12**: 1442.
14. Pfeiffer R, Simon F, Kuzmany H, Popov VN. *Phys. Rev.* 2005; **B72**: 161404(R).
15. Puech P, Hubel H, Dunstan DJ, Bassil A, Bacsa R, Peigney A, Flahaut E, Laurent C, Bacsa WS. *Phys. Stat. Sol. B* 2004; **241**(14): 3360.
16. Arvanitidis J, Christofilos D, Papagelis K, Andrikopoulos KS, Takenobu T, Iwasa Y, Kataura H, Ves S, Kourouklis GA. *Phys. Rev., B* 2005; **71**: 125404.
17. Chen G, Bandow S, Margine ER, Nisoli C, Kolmogorov AN, Crespi VH, Gupta R, Sumanasekera GU, Iijima S, Eklund PC. *Phys. Rev. Lett.* 2003; **90**: 257403.
18. Osswald S, Flahaut E, Ye H, Gogotsi Y. *Chem. Phys. Lett.* 2005; **402**: 422.
19. Kim Y, Muramatsu H, Kojima M, Hayashi T, Endo M, Terrones M, Dresselhaus MS. *Chem. Phys. Lett.* 2006; **420**: 377.
20. Corio P, Santos AP, Santos PS, Temperini MLA, Brar VW, Pimenta MA, Dresselhaus MS. *Chem. Phys. Lett.* 2004; **383**: 475.
21. Puech P, Flahaut E, Sapelkin A, Hubel H, Dunstan DJ, Landa G, Bacsa WS. *Phys. Rev., B* 2006; **73**: 233408.
22. Kürti J, Zólyomi V, Grüneis A, Kuzmany H. *Phys. Rev., B* 2002; **65**: 165433.
23. Wood JR, Zhao Q, Frogley MD, Meurs ER, Prins AD, Peijs T, Dunstan DJ, Wagner HD. *Phys. Rev., B* 2000; **62**: 7571.
24. O'Connell MJ, Eibergen EE, Doorn SK. *Nat. Mater.* 2005; **4**: 412.
25. Hulman M, Pfeiffer R, Kuzmany H. *New J. Phys.* 2004; **6**: 1.
26. Puech P, Bassil A, Gonzalez J, Power Ch, Flahaut E, Barrau S, Demont Ph, Lacabanne C, Perez E, Bacsa WS. *Phys. Rev., B* 2005; **72**: 155436.
27. Flahaut E, Durrieu MC, Remy-Zholgadri M, Bareille R, Baquey Ch. *Carbon* 2006; **44**(6): 1093.
28. Kim YA, Muramatsu H, Hayashi T, Endo M, Terrones M, Dresselhaus MS. *Chem. Phys. Lett.* 2004; **398**: 87.
29. Bassil A, Puech P, Tubery L, Bacsa W, Flahaut E. *Appl. Phys. Lett.* 2006; **88**: 173113.
30. Bandow S, Chen G, Sumanasekera GU, Gupta R, Iijima S, Eklund PC. *Phys. Rev.* 2002; **B66**: 075416.
31. Saito R, Grüneis A, Samsonidze GeG, Brar VW, Dresselhaus G, Dresselhaus MS, Jorio A, Cançado LG, Fantini C, Pimenta MA, Souza Filho AG. *New J. Phys.* 2003; **5**: 157.
32. Souza Filho AG, Jorio A, Swan AK, Unlu MS, Goldberg BB, Saito R, Hafner JH, Lieber CM, Pimenta MA, Dresselhaus G, Dresselhaus MS. *Phys. Rev.* 2002; **B65**: 085417.
33. Zhao Q, Wood JR, Wagner HD. *J. Polym. Sci., Part B: Polym. Phys.* 2001; **39**: 1492.
34. Sendova M, Flahaut E, DeBono B. *J. Appl. Phys.* 2005; **98**: 104304.
35. Bassil A, Puech P, Landa G, Bacsa W, Barrau S, Demont Ph, Lacabanne C, Perez E, Bacsa R, Flahaut E, Peigney A, Laurent Ch. *J. Appl. Phys.* 2005; **97**: 034303.
36. Thomsen C, Reich S. Raman scattering in carbon nanotubes. In *Light Scattering in Solids IX, Topics in Applied Physics*, Cardona M, Merlin R (eds). Springer Verlag: Heidelberg, 2006.
37. Sato K, Saito R, Oyama Y, Jiang J, Cançado LG, Pimenta MA, Jorio A, Samsonidze GeG, Dresselhaus G, Dresselhaus MS. *Chem. Phys. Lett.* 2006; **427**: 117.
38. Machon M. Electron-phonon Coupling, Vibrational, and Optical Properties of Carbon Nanotubes and Picotubes. PhD thesis, Berlin, Germany, 2006.
39. Bacsa WS, de Heer WA, Ugarte D, Châtelain A. *Chem. Phys. Lett.* 1993; **211**: 346.
40. Merlen A, Bendiab N, Toulemonde P, Aouizerat A, San Miguel A, Sauvajol JL, Montagnac G, Cardon H. *Phys. Rev., B* 2005; **72**: 035409.
41. Terrones M, Terrones H, Banhart F, Charlier J-C, Ajayan PM. *Science* 2000; **288**: 1226.
42. Loa I. *J. Raman Spectrosc.* 2003; **34**: 611.
43. Huang F, Yue KT, Tan P, Zhang SL, Shi Z, Zhou X, Gu Z. *J. Appl. Phys.* 1998; **84**: 4022.
44. Li HD, Yue T, Lian ZL, Zhou LX, Zhang SL, Shi ZJ, Gu ZN, Liu BB, Yang RS, Zou GT, Zhang Y, Iijima S. *Appl. Phys. Lett.* 2000; **76**: 2053.
45. Ci L, Zhou Z, Song L, Yan X, Liu D, Yuan H, Gao Y, Wang J, Liu L, Zhou W, Wang G, Xie S. *Appl. Phys. Lett.* 2003; **82**: 3098.
46. Thomsen C, Reich S, Jantoljak H, Loa I, Syassen K, Burghard M, Duesberg GS, Roth S. *Appl. Phys. A* 1999; **69**: 309.
47. Sandler J, Shaffer MSP, Windle AH, Halsall MP, Montes-Moran MA, Cooper CA, Young RJ. *Phys. Rev., B* 2003; **67**: 035417.
48. Hanfland M, Beister H, Syassen K. *Phys. Rev., B* 1989; **39**: 12598.
49. Tan P, Deng Y, Zhao Q, Cheng WC. *Appl. Phys. Lett.* 1999; **74**: 1818.
50. Rols S, Goncharenko IN, Almairac R, Sauvajol JL, Mirebeau I. *Phys. Rev., B* 2001; **64**: 153401.
51. Chan SP, Yim WL, Gong XG, Liu Chan ZF. *Phys. Rev., B* 2003; **68**: 075404.
52. Capaz R, Spataru C, Tangney P, Cohen M, Louie S. *Phys. Stat. Sol. B* 2004; **241**: 3352.
53. Amer MS, El-Ashry MM, Maguire JF. *J. Chem. Phys.* 2004; **121**: 2752.